Modeling turbulence in complex domains using explicit multi-scale forcing

A. K. Kuczaj[1] and B. J. Geurts[1,2]

[1] Department of Applied Mathematics and J.M. Burgers Center for Fluid Dynamics - University of Twente, P.O. Box 217, 7500 AE Enschede, The Netherlands, a.k.kuczaj@utwente.nl
[2] Department of Applied Physics - Eindhoven University of Technology, P.O. Box 513, 5300 MB Eindhoven, The Netherlands

Abstract: A new computational framework for the numerical simulation of turbulent flows through complex domains and along irregular boundaries is presented. The geometrical complexity is included by introducing explicit fractal forcing. This involves the agitation of a spectrum of length-scales and forms an integral part of the flow modeling. The potential application of such a modeling approach is illustrated by the evaluation of the turbulent mixing of a passive scalar field, driven by this turbulent flow. The surface-area and wrinkling of level-sets of the scalar field are monitored showing the influence of the forcing localization on the mixing efficiency.

Keywords: turbulence, complex domains, multi-scale forcing, passive scalar mixing

1 Introduction

Various important multi-scale phenomena in turbulent flows are caused by the interactions between the flow and geometrically complex objects placed inside the flow-domain. The origin of the flow perturbations that arises on many different scales of motion comes from the geometrically complex boundaries as occur, e.g., in case of a flow through a porous region (Fig. 1a). In literature, two approaches are used to capture the influence of these perturbations. These incorporate either the explicit boundary modeling, precisely describing its intricate shape, or a rather general macroscopic approximation in terms of effective boundary conditions. However, these methods either suffer from a lack of incorporated scales or are computationally not feasible.

We propose a different modeling approach to flows which undergo simultaneous perturbation over a broad range of scales by the interaction with a geometrically complicated object. The emergence of self-similar spectra in turbulence which do not follow the well known Kolmogorov $-5/3$ slope [1] was observed experimentally in flows over tree canopies [2]. This motivated us

to adopt explicit multi-scale fractal forcing [3] which captures the dominant geometrical complexities of the flow domain. In fractal forcing, turbulence is forced over a whole range of length-scales in a way that mimics a power-law forcing in spectral space (Fig. 1b). This offers the possibility of modeling the dynamic consequences of complex domain boundaries without the need to explicitly account for their intricate geometrical shape. The simultaneous disturbance of the flow over a spectrum of length-scales is approximated by a broad-band distribution of forcing intensities. This method can also incorporate cases in which only part of the domain is occupied by a complex obstruction, as sketched in Fig. 1c. In fact, by introducing an 'indicator' function to locate the complex object within the flow domain, the forcing can accommodate such spatial localization. This way the method could be used for global modeling of complicated geometry flows. However, a proper development of this methodology requires extensive examination of the influence of forcing on the energy dynamics, the spatial structures and the flow characteristics.

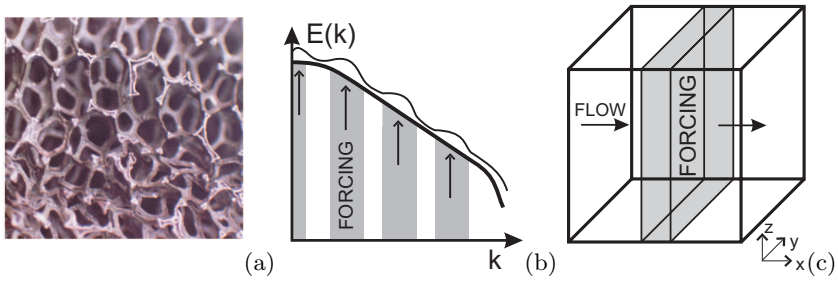

Fig. 1. Modeling of fluid flow through a complex geometry: a) porous metal sponge, b) multi-scale forcing in spectral space, c) spatial localization of forcing.

The aim of this paper is to present the general framework of multi-scale forced turbulence simulations. Forcing in computational models of turbulence has been solely directed toward maintaining a quasi-stationary state. It allows a study of inertial range dynamics corresponding to the classical Kolmogorov theory. We extend the application of such explicit forcing to simultaneously perturb the flow over a wide spectrum of length- and time-scales. Specifically, we consider the incompressible Navier-Stokes equations with the fractal forcing working as a stirrer controlled by its strength and size of disturbed scales. This computational modeling is illustrated with passive scalar mixing in the forced turbulent flow. Special attention is devoted to the mixing efficiency of a tracer by monitoring the surface area, curvature and wrinkling of level-sets of the scalar fields. The changes in mixing efficiency caused by the broad-band forcing are directly quantified using the level-set method developed in [4]. The application of broad-band forcing leads to distortion of the classical Kolmogorov energy spectrum picture reminiscent of a spectral

short-cut feature observed experimentally [2]. The production of additional large- and small-scale flow-features by the forcing enhances wrinkling and surface-area growth which plays an important role in turbulent mixing.

The organization of this paper is as follows. The Navier-Stokes equations and the passive scalar transport are briefly presented in §2 within our new framework. The results illustrating the possible application of broad-band forcing are collected in §3 with concluding remarks in §4.

2 Forced turbulence and passive scalar transport

Turbulence is described by the non-dimensional incompressible Navier-Stokes equations which govern the evolution of velocity $\mathbf{u}(\mathbf{x},t)$ and reduced pressure $p(\mathbf{x},t)$ subject to an external forcing $\mathbf{F}(\mathbf{x},t)$. The evolution obeys:

$$\begin{cases} \partial_t \mathbf{u}(\mathbf{x},t) + (\mathbf{u}(\mathbf{x},t)\cdot\nabla)\mathbf{u}(\mathbf{x},t) = -\nabla p(\mathbf{x},t) + Re^{-1}\nabla^2\mathbf{u}(\mathbf{x},t) + \mathbf{F}(\mathbf{x},t), \\ \nabla\cdot\mathbf{u}(\mathbf{x},t) = 0, \end{cases} \tag{1}$$

where Re is the Reynolds number. The equation for the passive scalar $T(\mathbf{x},t)$ has the form:

$$\partial_t T(\mathbf{x},t) + (\mathbf{u}(\mathbf{x},t)\cdot\nabla)T(\mathbf{x},t) = (ScRe)^{-1}\nabla^2 T(\mathbf{x},t). \tag{2}$$

The non-dimensional molecular diffusivity is denoted by $1/(ScRe)$ in terms of the product of the Schmidt (Sc) and Reynolds numbers. Applying the Fourier transform $\mathcal{F}$ and using the incompressibility constraint we obtain the following system of equations for the Fourier-coefficients of the velocity ($\widehat{\mathbf{u}}$) and scalar fields ($\widehat{T}$) [5]:

$$\begin{cases} \left(\partial_t + Re^{-1}k^2\right)\widehat{\mathbf{u}}(\mathbf{k},t) + \widehat{\mathbf{W}}(\mathbf{k},t) = \widehat{\mathbf{F}}(\mathbf{k},t), \\ \left(\partial_t + (ScRe)^{-1}k^2\right)\widehat{T}(\mathbf{k},t) + \widehat{Z}(\mathbf{k},t) = 0, \end{cases} \tag{3}$$

where $k = |\mathbf{k}|$ denotes the length of the wavevector $\mathbf{k}$. The nonlinear term $\widehat{\mathbf{W}}(\mathbf{k},t) = \mathcal{F}\left[(\mathbf{u}(\mathbf{x},t)\cdot\nabla)\mathbf{u}(\mathbf{x},t) + \nabla p(\mathbf{x},t)\right]$ and the convective term $\widehat{Z}(\mathbf{k},t) = \mathcal{F}\left[(\mathbf{u}(\mathbf{x},t)\cdot\nabla)T(\mathbf{x},t)\right]$ are computed pseudo-spectrally which involves transforming them back to the physical space to perform the products [6]. Beside the computational advantage of the Fourier expansion in periodic domains, this representation of the solution directly identifies the different length-scale contributions. This decomposition is helpful in the forcing definition presented next.

We used a slightly modified fractal forcing compared to the one proposed in [3]. The interactions of a fluid with a truncated fractal-like object are approximated through the induced drag force caused by the contact of that object with the flow. A power-law dependence on wavenumber was derived in which it is assumed that the drag is proportional to the surface area which

causes the blockage effect of the fluid. This surface area scales with a coefficient β, connected to the fractal dimension D_f by $\beta = D_f - 2$ [3]:

$$\widehat{\mathbf{F}}(\mathbf{k},t) = k^{\beta}\hat{f}\widehat{\mathbf{e}}(\mathbf{k},t). \tag{4}$$

The unit vector $\widehat{\mathbf{e}}$ is constructed on the basis of velocity and vorticity Fourier coefficients:

$$\widehat{\mathbf{e}}(\mathbf{k},t) = \gamma\left[\frac{\widehat{\mathbf{u}}(\mathbf{k},t)}{|\widehat{\mathbf{u}}(\mathbf{k},t)|} + \imath\frac{\mathbf{k}\times\widehat{\mathbf{u}}(\mathbf{k},t)}{|\mathbf{k}||\widehat{\mathbf{u}}(\mathbf{k},t)|}\right], \tag{5}$$

where γ is the normalization parameter to satisfy $|\mathbf{e}|^2 = 1$. The strength of the forcing term is controlled by specifying the desired energy input rate ε_w distributed over the set of forced modes $\mathbb{K}_F$ expressed by:

$$\hat{f} = \varepsilon_w / \sum_{\mathbb{K}_F} k^{\beta}\,|\widehat{\mathbf{u}}(\mathbf{k},t)|. \tag{6}$$

To solve (3) we used the four-stage compact-storage Runge-Kutta method [7]. The spectral discretization was fully dealiased by spectral truncation and a phase shift scheme. We applied exact integration of the viscous and diffusive terms [6]. To illustrate and quantify the influence of the fractal forcing on the turbulent dispersion of a passive scalar field we adopted the level-set integration method proposed in [4]. This method allows to determine, e.g., the surface-area, curvature and wrinkling of scalar level-sets. To quantify the evolving scalar level-set we may monitor its surface-area or surface-wrinkling. The latter is obtained by integrating $|\nabla\cdot\mathbf{n}|$ over the scalar level-set, with $\mathbf{n}$ the unit normal vector on that set. To present the application of the explicit broad-band forcing method along with the adopted procedure for the passive scalar evaluation we performed some relatively simple idealized numerical experiments which will be presented in the next section.

3 Forcing and mixing efficiency

In this section we first show the results of applying broad-band forcing in turbulence. Then, we turn to turbulent passive scalar mixing discussing briefly the influence of forcing on mixing time and mixing quality.

We performed numerical simulations at Reynolds number $Re = 1067$ where the length and time scales are defined by the size of the computational box $L = 1$ and the energy input rate ε_w. The resolution requirements were satisfactorily fulfilled as $k_{max}\eta$ ranges from 2.3 to 3.5 (η - Kolmogorov scale) using a resolution of 128^3 and 192^3 grid-cells, which yields after dealiasing 60 and 90 'active' wavenumbers, respectively. For the passive scalar with $Sc = 0.7$ used in the simulations this gives $k_{max}\eta_{OC} = 3.0\ldots4.5$ (η_{OC} - Obukhov-Corrsin scale). The fractal dimension used in the simulations was $D_f = 2.6$ yielding a surface area scaling $\beta = 0.6$. The wavenumbers were rescaled by $L/(2\pi)$.

As a reference point we used large-scale forcing with $\varepsilon_w = 0.15$ which keeps the system energetically in a quasi-stationary state. We refer to this as case A15 in which the forced modes are $\mathbb{K}_F : k \leq 1.5$. The application of additional perturbation to the flow in higher wavenumber bands produces more spatial scales which change the characteristics of the transport. To study this influence we specified two regions where we applied supplementary fractal forcing with $\varepsilon_w = 0.45$. The first region is situated near the largest scales of the flow ($B45_1$ case - $\mathbb{K}_F : 4.5 < k \leq 8.5$) and the second one at some distance from the largest scales ($B45_2$ case - $\mathbb{K}_F : 12.5 < k \leq 16.5$) to enhance even smaller scales. Finally, we also considered mixing in case $\varepsilon_w = 0.6$ in the large scales only (A60 case - $\mathbb{K}_F : k \leq 1.5$).

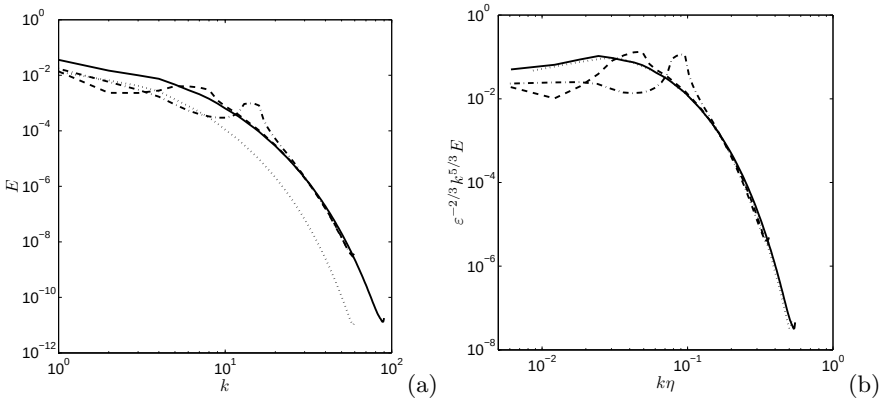

Fig. 2. Energy spectrum: a) $E(k)$, b) $\varepsilon^{-2/3}k^{5/3}E(k)$ for A60 (solid), $B45_1$ (dashed) and $B45_2$ (dash-dotted), A15 (dotted).

The energy spectra averaged over 10 independent realizations of the initial condition and over a time-interval of 10 eddy-turnover times are presented in Fig. 2. Time-averaging was started after allowing the flow to develop for 5 eddy-turnover times. The additional energy input in the higher wavenumber bands causes a nonlocal modulation in the energy spectrum. This leads to a different dynamics of the flow (Fig. 2a). There is a clear cross-over in the spectra of the broad-band forced cases. At low wavenumber the spectra coincide with the A15 case while at high wavenumbers the tails overlap the A60 case. Rescaling the energy and length-scales yields Fig. 2b. This gives information about the energy distribution over the different scales. Broad-band forcing is seen not to lead to a significant change in the total energy present in the flow. Mainly the high-k forcing changes the distribution of energy over the scales of motion. Specifically, broad-band forcing produces smaller scales and in this way the dissipation of energy increases. The energy is present in different scales of motion and by changing the strength and spatial location

of the forcing, we have the possibility to control its distribution and hence its transport properties.

We next consider the consequences of the different forcing strategies for the efficiency with which the passive scalar is stirred. The nature of stirring comes from the convective turbulent flow properties which drive the scalar while on the other hand mixing is strongly influenced by molecular diffusion. These two physical mechanisms work simultaneously and are responsible for the final result which is commonly called 'mixing'. To study turbulent mixing properties we simulated the spreading of a passive tracer at the earlier mentioned Schmidt number of 0.7. Initially, we start with a spherical distribution of tracer of radius 3/16 with the radial distribution as a step function softened by a Gaussian profile at the edge and internal concentration equal one.

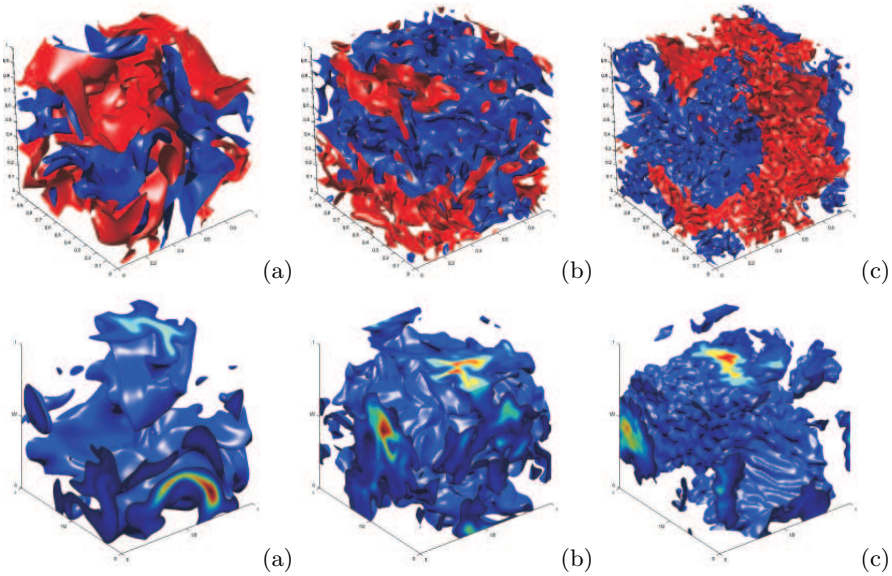

Fig. 3. Snapshot of velocity field iso-surfaces (above) and passive scalar concentration (below) at $t = 0.5$ for: a) A15, b) $B45_1$, c) $B45_2$.

The changes in the flow properties in the different cases have consequences for the quality of mixing as we can observe in Fig. 3. Consistent with the length-scale ranges that are forced we observe more small-scale features in the velocity fields and correspondingly more localized 'wrinkling' of the level-sets of the passive scalar. To quantify this first impression given by these snapshots we define the growth parameter of the surface-area $A(t)$ at time t of the selected level-set as $\vartheta_A(t) = A(t)/A(0)$. Similarly, we may monitor the growth ϑ_W of the surface-wrinkling $W(t)$.

We obtain an enhancement of the mixing for the broad-band cases ($B45_1$, $B45_2$) compared to the large scale forcing case at $\varepsilon_w = 0.15$ (A15). The mixing is more efficient not only in terms of the quality as indicated by the maxima of the individual curves in Fig. 4a, but also in terms of the time needed to reach a similar level of mixing. Comparing the different cases, similar levels of surface-area are obtained in about half the time for the broad-band forced cases. So, 'investing' extra energy by agitating high-k bands does produce additional mixing. However, if we compare these results to the energetically equally costly A60 case with energy inserted only in the low-k band then the situation is quite different. The growth parameter for the area reaches its maximum value both sooner and at a higher value. This can be explained because the ratio of the initial tracer volume and the whole computational domain is $1 : 36$ and the Schmidt number is comparatively small. Convective spreading of the tracer dominates over the decay caused by molecular diffusion and, hence, larger scales play a crucial role.

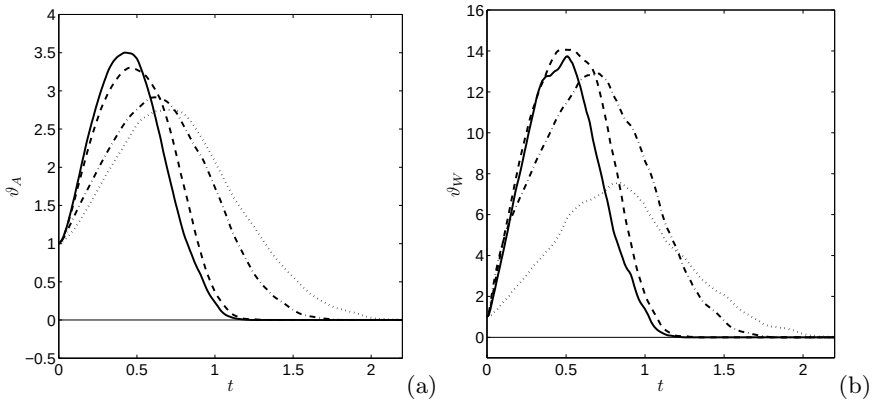

Fig. 4. Evolution of decaying passive scalar: a) area, b) wrinkling. Growth parameter $\vartheta_A(t)$ and $\vartheta_W(t)$ at the level-set 0.25 for A60 (solid), $B45_1$ (dashed), $B45_2$ (dash-dotted) and A15 (dotted).

In many cases, e.g., in combustion processes not only the surface-area but other quantities like the small-scale wrinkling are important to keep the chemical reactions at an optimum level. The wrinkling growth parameter in Fig. 4b is in general a measure of the average local surface complexity. It exhibits a maximal value for the broad-band forcing situated near the largest scales. The higher band forcing needs to compete more directly with the viscous effects and it was found less effective in producing surface-area, which is more related to 'sweeping' motions over 'reasonable' distances. In contrast we observe here that more localized distortions of the scalar level-sets are less affected by this competition with viscosity. The level-set integration method is

effective in quantifying these general impressions. This may help to identify optimal stirring procedures to which future research will be devoted.

4 Conclusions

We presented a methodology for the numerical investigation of turbulent flow which undergoes simultaneous forcing over a broad range of scales as a result of interaction with complex domain boundaries. We have shown that with a relatively simple model we can mimic some basic properties of very complex flows. The application of fractal forcing causes an enhancement of energy dissipation in the system producing the so-called spectral short-cut feature observed experimentally [2].

The passive scalar field driven by the forced flow was examined using a level-set evaluation approach to quantify basic general characteristics of mixing quality and efficiency. We illustrated it by performing numerical simulations of a tracer decay in turbulence forced at different length-scales. The results show successful application of the evaluation method in searching an optimal state between surface area and its wrinkling needed in many technological processes. Specifically, it was found that broad-band forcing causes additional production of smaller scales in the flow and for a small initial size of a tracer and Schmidt number this effect is directly responsible for the wrinkling area enhancement, while the surface area of a tracer is mainly governed by the large-scales in this case.

The natural extension of the presented method will be the use of passive scalar forcing and the spatial localization of the broad-band forcing region to which future attention will be given.

Acknowledgments

This work is part of the research program "Turbulence and its role in energy conversion processes" of the Foundation for Fundamental Research of Matter (FOM). The authors wish to thank the SARA Computing and Networking Services in Amsterdam for providing the computational resources.

References

1. Kolmogorov A.N. (1941) C.R. Acad. Sci. URSS, 30:301–305
2. Finnigan J. (2000) Ann. Rev. Fluid Mech., 32:519–571
3. Mazzi B., Vassilicos J.C. (2004) J. Fluid Mech., 502:65–87
4. Geurts B.J. (2001) JoT, 2(17):2–24
5. McComb W.D. (1991) Physics of Fluid Turbulence, Oxford University Press
6. Canuto C., et al. (1988) Spectral Methods in Fluid Dynamics, Springer Verlag
7. Geurts B.J. (2003) Elements of direct and large-eddy simulation, R.T. Edwards